

Control of Power Kites for Naval Propulsion

L. Fagiano*, M. Milanese*, V. Razza*

Abstract—This paper investigates the application of an innovative technology for high–altitude wind power generation to naval propulsion. The basic idea is to exploit the traction forces exerted by automatically controlled power kites, flying fast in crosswind conditions, to pull a boat. Numerical analyses are carried out employing a mathematical model of the system and an efficient Nonlinear Model Predictive Control (NMPC) law. Differently from existing approaches, the cost function considered in NMPC design is directly the predicted traction force exerted on the kite lines. The obtained numerical results are compared with the data collected during experimental tests carried out in the project KiteNav, undergoing at Politecnico di Torino.

I. INTRODUCTION

During the last five years, several studies (see e.g. [1], [2]) have been devoted to develop technologies for high–altitude wind energy generation using controlled tethered airfoils. The basic idea is to capture wind energy using airfoils (e.g. power kites used for surfing or sailing), linked to the ground by one or two cables, whose flight is suitably driven by an automatic control unit. Wind energy is collected at ground level by converting the mechanical power transferred by the kite lines into electrical power, using a suitable mechanism and electric generators. This class of power generators is able to exploit wind flows at higher altitudes (up to 1000 m) than the actual wind technology, where quite strong and constant wind can be found basically everywhere in the world.

In this paper, the focus is on the application of the concept of high–altitude wind power using controlled power kites to naval propulsion, instead of electricity generation. The use of tethered airfoils to tow a boat brings several advantages with respect to classical sails, due to the possibility for the airfoil to reach stronger winds blowing at higher altitudes and to fly fast in crosswind direction, thus generating surprisingly high force values. Indeed, this idea is currently being developed and industrialized by some companies around the world, like SkySails GmbH [3]. Moreover, the potential of a kite boat system similar to the one of [3] has been investigated in [4], considering the problem of computing kite orbits that are optimal with respect to the traction forces. In this work, a small boat is considered (i.e. a 38–feet–long yacht), equipped with a small–scale high–altitude wind power generator. In the system configuration considered here, the kite is linked with two cables to the boat, instead of the single cable considered in [3], [4]. This way, the kite can be controlled

by differentially pulling the lines via actuators placed on the boat and avoiding the use of wireless actuators on the airfoil. Moreover, in the case of breaking of one cable, the presence of two lines makes it possible to recover both the airfoil and the lines. Thus, the configuration considered in this paper appears to be safer than the one of [3], [4]. Automatic control is the key point in this application, since the system to be controlled is nonlinear, open–loop unstable and subject to hard operational constraints. In order to tackle such a challenging control problem, an efficient approximate Nonlinear Model Predictive Control (NMPC) law is used (see e.g. [5]). Differently from [2], [4], here the control law is designed in order to directly maximize the predicted traction force acting on the boat, without using any pre–computed optimal kite orbit. Numerical simulations using the designed NMPC law are performed to study the system behaviour and its robustness to wind turbulence. Moreover, the obtained numerical results are compared with the first experimental data, collected during field tests performed near Genoa, Italy, in order to evaluate the matching between real world measures and simulation results.

II. SYSTEM DESCRIPTION AND MODEL EQUATIONS

A. System description

In the considered application of high–altitude wind power to naval propulsion, the kite is connected to the boat by two cables (see Fig. 1(a)), realized in composite materials, with a traction resistance 8–10 times higher than that of steel cables of the same weight. The cables are rolled around two drums, linked to two electric drives which are able to act both as generators and as motors. An electronic control system can drive the kite flight by differentially pulling the cables. The kite flight is tracked and controlled using on–board wireless instrumentation (GPS, magnetic and inertial sensors) as well as ground sensors, to measure the airfoil speed and position, the power output, the cable force and speed and the wind speed and direction. The system composed by the electric drives, the drums, and all the hardware needed to control a single kite is denoted as Kite Steering Unit (KSU, see Fig. 1(b)). The next Section presents the mathematical model employed to describe the dynamical behaviour of the system.

B. Model equations

A Cartesian coordinate system (X, Y, Z) is considered (see Fig. 2), centered at the boat location (i.e. at the KSU, which is fixed with respect to the boat), with X axis aligned with the longitudinal symmetry axis of the boat. Wind speed vector is denoted as $\vec{W}_l = \vec{W}_0 + \vec{W}_t$, where \vec{W}_0 is the nominal wind,

This research was partly supported by funds of Regione Piemonte, Italy, under the Project “KiteNav: power kites for naval propulsion”. Project partners: Politecnico di Torino, Azimut–Benetti s.p.a. and Modelway s.r.l.

*Politecnico di Torino, Dipartimento di Automatica e Informatica, Corso Duca degli Abruzzi 24 – 10129 Torino – Italy

e–mail addresses: lorenzo.fagiano@polito.it, mario.milanese@polito.it, valentino.razza@polito.it

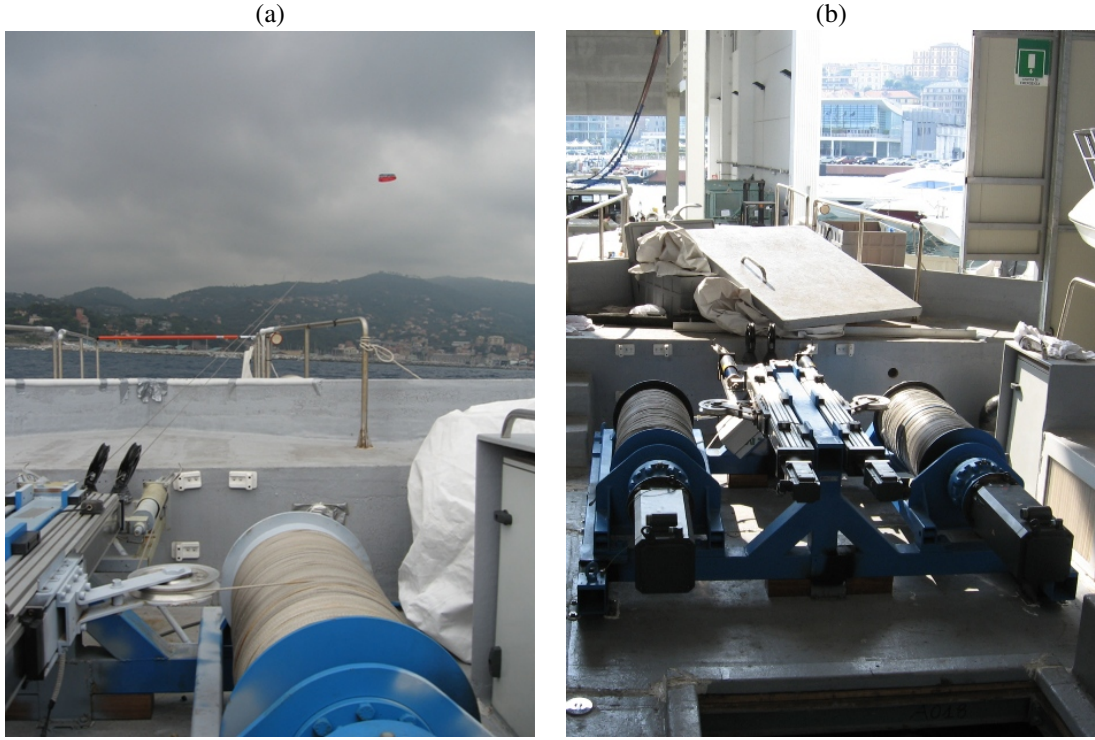


Fig. 1. (a) Prototype of high-altitude wind power generator for naval propulsion operating near Genoa, Italy. (b) Kite Steering Unit installed on the prototype.

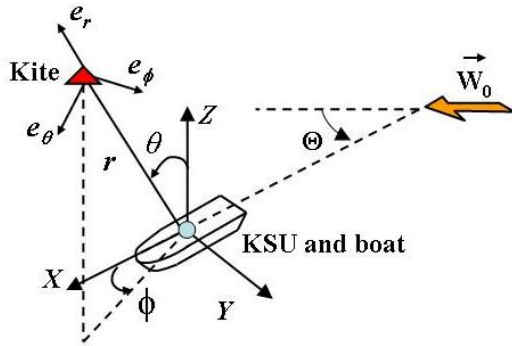


Fig. 2. Model diagram of the system.

supposed to be known and expressed in (X, Y, Z) as:

$$\vec{W}_0 = \begin{pmatrix} W_n(Z) \cos(\Theta) \\ -W_n(Z) \sin(\Theta) \\ 0 \end{pmatrix} \quad (1)$$

Θ is the angle between the nominal wind speed direction and X axis, while $W_n(Z)$ is a known function which gives the nominal wind magnitude at the altitude Z . In this paper, function $W_n(Z)$ corresponds to a wind shear model (see e.g. [6]), which has been identified using the data contained in the database RAOB (RAwinsonde OBServation) of the National Oceanographic and Atmospheric Administration, see [7]. An example of winter and summer wind shear profiles related to the site of Cagliari in Italy is reported in Fig. 3. The term \vec{W}_i may have components in all directions and is not supposed

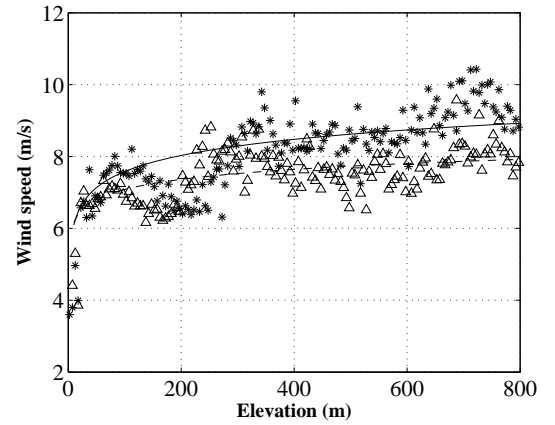


Fig. 3. Wind shear model related to the site of Cagliari, in Italy, for winter months (model: solid line, measured data: asterisks) and for summer months (model: dashed line, measured data: triangles)

to be known, accounting for wind unmeasured turbulence. In system (X, Y, Z) , the kite position can be expressed as a function of its distance r from the origin and of the two angles θ and ϕ , as depicted in Fig. 2, which also shows the three unit vectors e_θ , e_ϕ and e_r of a local coordinate system centered at the kite center of gravity. Unit vectors (e_θ, e_ϕ, e_r) are expressed in the Cartesian system (X, Y, Z)

by:

$$\begin{pmatrix} e_\theta & e_\phi & e_r \end{pmatrix} = \begin{pmatrix} \cos(\theta) \cos(\phi) & -\sin(\theta) \cos(\phi) & \sin(\theta) \cos(\phi) \\ \cos(\theta) \sin(\phi) & \cos(\phi) & \sin(\theta) \sin(\phi) \\ -\sin(\theta) & 0 & \cos(\theta) \end{pmatrix} \quad (2)$$

The dynamical equations of motion of the boat and of the kite will be now briefly resumed.

1) *Boat model*: the following assumptions are considered:

- the boat rudder is commanded in such a way that the boat speed vector \vec{v} is aligned with axis X ;
- the boat moves along a straight path;
- the effects of the lateral forces exerted by the cables on the boat are negligible and/or balanced by a suitable action on the rudder.

According to such assumptions, the angular speed $\dot{\Theta}$ is zero or negligible. The considered assumptions are reasonable in the context of this paper and allow to describe with satisfactory accuracy the longitudinal motion of the boat pulled by the kite lines, which is of interest in this work. Since the speed vector \vec{v} is supposed to be aligned with axis X , its direction with respect to the nominal wind speed direction is univocally defined by angle Θ . Thus, in the following the boat speed will be described simply by its magnitude v . On the basis of the considered assumptions, the boat model is given by the following equation:

$$\dot{v} = \frac{F^{c, \text{trc}} \sin(\theta) \cos(\phi) - F^R(v)}{M} \quad (3)$$

where M is the boat mass, $F^{c, \text{trc}}$ is the traction force exerted by the lines on the boat (see Section II-B.2) and $F^R(v)$ is the longitudinal drag force acting on the boat moving at a given speed v . Function $F^R(v)$ can be identified through experimental tests on the boat; in this paper the following form is considered:

$$F^R(v) = R_4 v^4 + R_3 v^3 + R_2 v^2 + R_1 v \quad (4)$$

where $R_4 = 56.9$, $R_3 = -130.7$, $R_2 = 256.9$ and $R_1 = 165.4$. Such values have been identified through tests on the real boat employed in the KiteNav project, built by the project partner Azimut-Benetti s.p.a., and can be considered valid for boat speed values ranging from 0 m/s to 5 m/s.

2) *Airfoil's model*: applying Newton's laws of motion to the kite in the local coordinate system (e_θ, e_ϕ, e_r) , the following dynamic equations are obtained:

$$\begin{aligned} \ddot{\theta} &= \frac{F_\theta}{m r} \\ \ddot{\phi} &= \frac{F_\phi}{m r \sin \theta} \\ \ddot{r} &= \frac{F_r}{m} \end{aligned} \quad (5)$$

where m is the kite mass. Forces F_θ , F_ϕ and F_r include the contributions of gravity force \vec{F}^{grav} of the kite and the lines, apparent force \vec{F}^{app} , kite aerodynamic force \vec{F}^{aer} , aerodynamic drag force $\vec{F}^{\text{c, aer}}$ of the lines and traction

force $F^{c, \text{trc}}$ exerted by the lines on the kite. Their relations, expressed in the local coordinates (e_θ, e_ϕ, e_r) are given by:

$$\begin{aligned} F_\theta &= F_\theta^{\text{grav}} + F_\theta^{\text{app}} + F_\theta^{\text{aer}} + F_\theta^{\text{c, aer}} \\ F_\phi &= F_\phi^{\text{grav}} + F_\phi^{\text{app}} + F_\phi^{\text{aer}} + F_\phi^{\text{c, aer}} \\ F_r &= F_r^{\text{grav}} + F_r^{\text{app}} + F_r^{\text{aer}} + F_r^{\text{c, aer}} - F^{c, \text{trc}} \end{aligned} \quad (6)$$

Each force contribution will be now briefly described.

Gravity forces. The magnitude of the overall gravity force applied to the kite center of gravity is the sum of the kite weight and the contribution $F^{c, \text{grav}}$ given by the weight of the lines. Assuming that the weight of each line is applied at half its length (i.e. $r/2$), $F^{c, \text{grav}}$ can be computed considering the rotation equilibrium equation around the point where the lines are attached to the KSU:

$$\frac{r \cos(\theta)}{2} \frac{2 \rho_l \pi d_l^2 r}{4} g = F^{c, \text{grav}} r \cos(\theta) \quad (7)$$

where g is the gravity acceleration, ρ_l is the line material density and d_l is the diameter of each line. Thus, the magnitude of the overall gravity force \vec{F}^{grav} can be computed as:

$$|\vec{F}^{\text{grav}}| = m g + F^{c, \text{grav}} = \left(m + \frac{\rho_l \pi d_l^2 r}{4} \right) g \quad (8)$$

Vector \vec{F}^{grav} in the fixed coordinate system (X, Y, Z) is directed along the negative Z direction. Thus, using the rotation matrix (2) the following expression is obtained for the components of \vec{F}^{grav} in the local coordinates (e_θ, e_ϕ, e_r) :

$$\vec{F}^{\text{grav}} = \begin{pmatrix} F_\theta^{\text{grav}} \\ F_\phi^{\text{grav}} \\ F_r^{\text{grav}} \end{pmatrix} = \begin{pmatrix} \left(m + \frac{\rho_l \pi d_l^2 r}{4} \right) g \sin(\theta) \\ 0 \\ - \left(m + \frac{\rho_l \pi d_l^2 r}{4} \right) g \cos(\theta) \end{pmatrix} \quad (9)$$

Apparent forces. Assuming little acceleration \dot{v} of the boat, the components of vector \vec{F}^{app} result to be:

$$\begin{aligned} F_\theta^{\text{app}} &= m(\dot{\phi}^2 r \sin \theta \cos \theta - 2\dot{r}\dot{\theta}) \\ F_\phi^{\text{app}} &= m(-2\dot{r}\dot{\phi} \sin \theta - 2\dot{\phi}\dot{r} \cos \theta) \\ F_r^{\text{app}} &= m(r\dot{\theta}^2 + r\dot{\phi}^2 \sin^2 \theta) \end{aligned} \quad (10)$$

Kite aerodynamic forces. The aerodynamic force \vec{F}^{aer} depends on the effective wind speed \vec{W}_e , which in the local system (e_θ, e_ϕ, e_r) is computed as:

$$\vec{W}_e = \vec{W}_l - \vec{W}_a \quad (11)$$

where \vec{W}_a is the kite speed with respect to the ground, which can be expressed in the local coordinate system (e_θ, e_ϕ, e_r) as:

$$\vec{W}_a = \begin{pmatrix} \dot{\theta} r + v \cos(\theta) \cos(\phi) \\ \dot{\phi} r \sin \theta - v \sin(\phi) \\ \dot{r} + v \sin(\theta) \cos(\phi) \end{pmatrix} \quad (12)$$

Let us consider now the kite wind coordinate system $(\vec{x}_w, \vec{y}_w, \vec{z}_w)$ (Fig. 4(a)–(b)), with the origin in the kite center of gravity, \vec{x}_w basis vector aligned with the effective wind speed vector, pointing from the trailing edge to the leading edge of the kite, \vec{z}_w basis vector contained in the kite

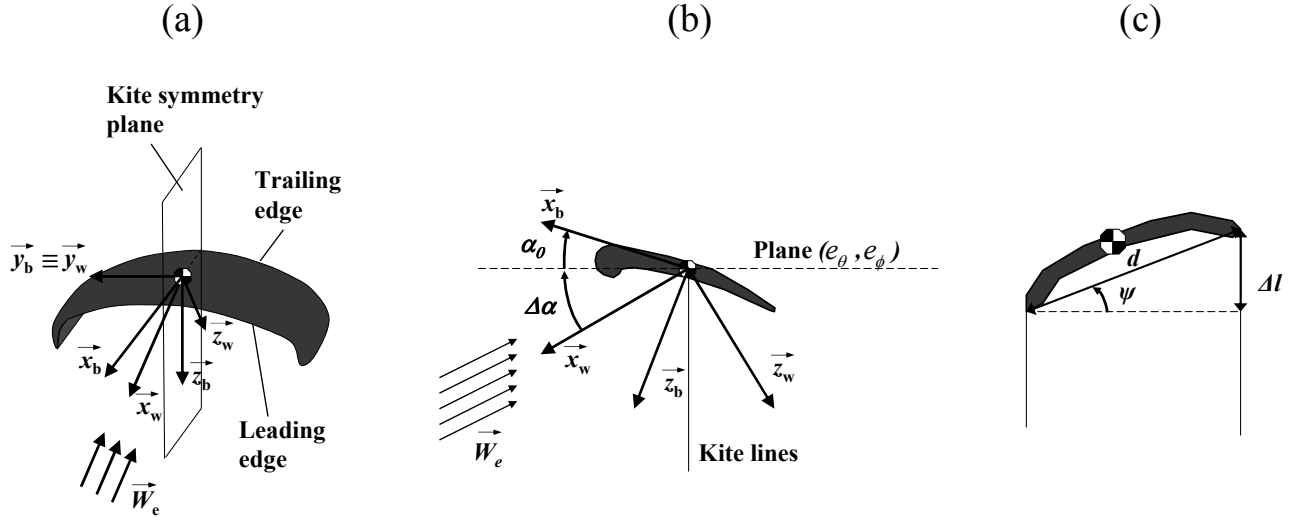


Fig. 4. (a) Scheme of the kite wind coordinate system $(\vec{x}_w, \vec{y}_w, \vec{z}_w)$ and body coordinate system $(\vec{x}_b, \vec{y}_b, \vec{z}_b)$. (b) Wind axes (\vec{x}_w, \vec{z}_w) , body axes (\vec{x}_b, \vec{z}_b) and angles α_0 and $\Delta\alpha$. (c) Command angle ψ

symmetry plane and pointing from the top surface of the kite to the bottom and wind \vec{y}_w basis vector completing the right handed system. Unit vector \vec{x}_w can be expressed in the local coordinate system (e_θ, e_ϕ, e_r) as:

$$\vec{x}_w = -\frac{\vec{W}_e}{|\vec{W}_e|} \quad (13)$$

According to [8], vector \vec{y}_w can be expressed in the local coordinate system (e_θ, e_ϕ, e_r) as:

$$\vec{y}_w = e_w(-\cos(\psi)\sin(\eta)) + (e_r \times e_w)(\cos(\psi)\cos(\eta)) + e_r \sin(\psi) \quad (14)$$

where:

$$e_w = \frac{\vec{W}_e - e_r(e_r \cdot \vec{W}_e)}{|\vec{W}_e - e_r(e_r \cdot \vec{W}_e)|} \quad (15)$$

$$\eta = \arcsin\left(\frac{\vec{W}_e \cdot e_r}{|\vec{W}_e - e_r(e_r \cdot \vec{W}_e)|} \tan(\psi)\right)$$

Angle ψ is the control input, defined by

$$\psi = \arcsin\left(\frac{\Delta l}{d}\right) \quad (16)$$

with d being the distance between the two lines fixing points at the kite and Δl the length difference of the two lines (see Fig. 4(c)). Δl is considered positive if, looking the kite from behind, the right line is longer than the left one. Basically, angle ψ influences the kite motion by changing the direction of vector \vec{F}^{aer} . Finally, the wind unit vector \vec{z}_w can be computed as:

$$\vec{z}_w = \vec{x}_w \times \vec{y}_w \quad (17)$$

Then, the aerodynamic force \vec{F}^{aer} in the local coordinate system (e_θ, e_ϕ, e_r) is given by:

$$\vec{F}^{\text{aer}} = \begin{pmatrix} F_\theta^{\text{aer}} \\ F_\phi^{\text{aer}} \\ F_r^{\text{aer}} \end{pmatrix} = -\frac{1}{2} C_D A \rho |\vec{W}_e|^2 \vec{x}_w - \frac{1}{2} C_L A \rho |\vec{W}_e|^2 \vec{z}_w \quad (18)$$

where ρ is the air density, A is the kite characteristic area, C_L and C_D are the kite lift and drag coefficients. As a first approximation, the drag and lift coefficients are nonlinear functions of the kite angle of attack α . To define angle α , the kite body coordinate system $(\vec{x}_b, \vec{y}_b, \vec{z}_b)$ needs to be introduced (Fig. 4(a)–(b)), centered in the kite center of gravity with unit vector \vec{x}_b contained in the kite symmetry plane, pointing from the trailing edge to the leading edge of the kite, unit vector \vec{z}_b perpendicular to the kite surface and pointing down and unit vector \vec{y}_b completing a right-handed coordinate system. Such a system is fixed with respect to the kite. The attack angle α is then defined as the angle between the wind axis \vec{x}_w and the body axis \vec{x}_b (see Fig. 4(b)). Note that in the employed model, it is supposed that the wind axis \vec{x}_w is always contained in the kite symmetry plane. Moreover, it is considered that by suitably regulating the attack points of the lines to the kite, it is possible to impose a desired *base* angle of attack α_0 to the kite: such an angle (depicted in Fig. 4(b)) is defined as the angle between the kite body axis \vec{x}_b and the plane defined by local vectors e_θ and e_ϕ , i.e. the tangent plane to a sphere with radius r . Then, the actual kite angle of attack α can be computed as the sum of α_0 and the angle $\Delta\alpha$ between the effective wind \vec{W}_e and the plane defined by (e_θ, e_ϕ) :

$$\alpha = \alpha_0 + \Delta\alpha$$

$$\Delta\alpha = \arcsin\left(\frac{e_r \cdot \vec{W}_e}{|\vec{W}_e|}\right) \quad (19)$$

Functions $C_L(\alpha)$ and $C_D(\alpha)$ employed in this paper are reported in Fig. 5 (see [1] for more details).

Line forces. The lines influence the kite motion through their weight (that has been already taken into account in the gravity forces), their drag force $\vec{F}^{\text{c, aer}}$ and the traction force $F^{\text{c, trc}}$. An estimate of the drag of the lines has been considered in [9], where the overall angular momentum $\vec{M}_d = r e_r \times \vec{F}^{\text{c, aer}}$ exerted by the line drag force is computed

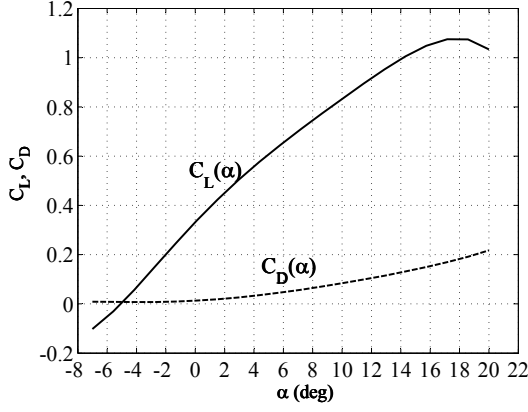


Fig. 5. Kite Lift coefficient C_L (solid) and drag coefficient C_D (dashed) as functions of the attack angle α .

by integrating, along the line length, the angular momentum given by the drag force acting on an infinitely small line segment:

$$\begin{aligned} \vec{M}_d &= \int_0^r \left(s e_r \times -\frac{\rho C_{D,l} d_l \cos(\Delta\alpha)}{2} \left(\frac{s |\vec{W}_e|}{r} \right)^2 \vec{x}_w \right) ds \\ &= r e_r \times -\frac{\rho C_{D,l} A_l \cos(\Delta\alpha)}{8} |\vec{W}_e|^2 \vec{x}_w \end{aligned} \quad (20)$$

where $C_{D,l}$ is the line drag coefficient and $A_l \cos(\Delta\alpha) = r d_l \cos(\Delta\alpha)$ is the projection of the line front area on the plane perpendicular to the effective wind vector (see [1] for details). The line drag force is then computed as:

$$\vec{F}^{\text{c,aer}} = \begin{pmatrix} F_{\theta}^{\text{c,aer}} \\ F_{\phi}^{\text{c,aer}} \\ F_r^{\text{c,aer}} \end{pmatrix} = -\frac{\rho C_{D,l} A_l \cos(\Delta\alpha)}{8} |\vec{W}_e|^2 \vec{x}_w \quad (21)$$

The traction force $F^{\text{c,trc}}$ is always directed along the local unit vector e_r and cannot be negative in equation (6), since the kite can only pull the lines. Moreover, $F^{\text{c,trc}}$ is measured by a force transducer on the KSU and, using a local controller of the electric drives, it is regulated in such a way that $\dot{r}(t) = 0$, i.e. a constant line length is employed to tow the boat.

3) *Overall model equations:* considering that the nominal wind speed magnitude $W_n(Z)$ can be obtained by computing the kite altitude Z as $Z = r \sin(\theta)$, equations (1)–(21) give the system dynamics in the form:

$$\dot{x}(t) = f(x(t), u(t), \Theta, \vec{W}_t(t)) \quad (22)$$

where $x(t) = [\theta(t) \ \phi(t) \ r(t) \ \dot{\theta}(t) \ \dot{\phi}(t) \ \dot{r}(t) \ v(t)]^T$ are the model states and $u(t) = \psi(t)$ is the control input. All the model states are measured using the available sensors placed on the kite and on the KSU. The model $f(\cdot)$ can be employed to design the control law and to simulate the system behaviour, as it will shown in the next Sections.

III. CONTROL DESIGN

The control problem and related objectives are now described. As highlighted in Section I, the control objective

is to maximize the traction force exerted by the cables on the boat along its path. In order to accomplish this aim while satisfying the constraints that are inherent in this problem, a Nonlinear Model Predictive Control strategy (NMPC, see e.g. [10]) is employed. In this framework, the control move computation is performed at discrete time instants defined on the basis of a suitably chosen sampling period Δ_t . At each sampling time $t_k = k\Delta_t$, $k \in \mathbb{N}$, the measured values of the state $x(t_k)$ and of the angle Θ between the nominal wind speed direction and the boat direction are used to compute the control move through the optimization of a performance index of the form:

$$J(U, t_k, T_p) = \int_{t_k}^{t_k+T_p} L(\tilde{x}(\tau), \tilde{u}(\tau), \Theta) d\tau \quad (23)$$

where $T_p = N_p \Delta_t$, $N_p \in \mathbb{N}$ is the prediction horizon, $\tilde{x}(\tau)$ is the state predicted inside the prediction horizon according to the state equation (22), using $\tilde{x}(t_k) = x(t_k)$ and the piecewise constant control input $\tilde{u}(t)$ belonging to the sequence $U = \{\tilde{u}(t)\}$, $t \in [t_k, t_k+T_p]$ defined as:

$$\tilde{u}(t) = \begin{cases} \bar{u}_i, \forall t \in [t_i, t_{i+1}], i = k, \dots, k+T_c-1 \\ \bar{u}_{k+T_c-1}, \forall t \in [t_i, t_{i+1}], i = k+T_c, \dots, k+T_p-1 \end{cases} \quad (24)$$

where $T_c = N_c \Delta_t$, $N_c \in \mathbb{N}$, $N_c \leq N_p$ is the control horizon.

The function $L(\cdot)$ in (23) is suitably defined on the basis of the performances to be achieved. In the considered problem, function $L(\cdot)$ is chosen as the towing force exerted by the cables on the boat, i.e.:

$$L(x, u, \Theta) = F^{\text{c,trc}} \sin(\theta) \cos(\phi)$$

Moreover, in order to take into account the existing physical limitations on both the kite flight and the control input ψ , constraints of the form $\tilde{x}(t) \in \mathbb{X}$, $\tilde{u}(t) \in \mathbb{U}$ have been included too. In particular, the following state constraint is considered to keep the kite sufficiently far from the ground:

$$\theta(t) \leq \bar{\theta} \quad (25)$$

with $\bar{\theta} < \pi/2$ rad. Actuator physical limitations give rise to the constraints:

$$\begin{aligned} |\psi(t)| &\leq \bar{\psi} \\ |\dot{\psi}(t)| &\leq \bar{\dot{\psi}} \end{aligned} \quad (26)$$

As a matter of fact, other technical constraints have been added to force the kite to go along “figure eight” trajectories rather than circular ones, in order to prevent the lines from wrapping one around the other. Such constraints force the kite ϕ angle to oscillate with double period with respect to θ angle, thus generating the proper kite trajectory.

The predictive control law is then computed using a receding horizon strategy:

- 1) At time instant t_k , get $x(t_k)$.
- 2) Solve the optimization problem:

$$\min_U J(U, t_k) \quad (27a)$$

$$\text{subject to} \quad (27b)$$

$$\tilde{x}(t_k) = x(t_k) \quad (27c)$$

$$\dot{\tilde{x}}(t) = f(\tilde{x}(t), \tilde{u}(t), \Theta) \forall t \in (t_k, t_k+T_p] \quad (27d)$$

$$\tilde{x}(t) \in \mathbb{X}, \tilde{u}(t) \in \mathbb{U} \forall t \in [t_k, t_k+T_p] \quad (27e)$$

- 3) Apply the first element of the solution sequence U to the optimization problem as the actual control action $u(t_k) = \tilde{u}(t_k)$.
- 4) Repeat the whole procedure at the next sampling time t_{k+1} .

The NMPC law results to be a nonlinear static function of the system state x , and the boat direction Θ w.r.t. the nominal wind direction:

$$\psi(t_k) = \kappa(x(t_k), \Theta) = \kappa(w(t_k)) \quad (28)$$

As a matter of fact, an efficient NMPC implementation is required to ensure that the control move is computed within the employed sampling time, of the order of 0.2 s. This can be obtained using e.g. the Fast Model Predictive Control (FMPC) techniques introduced and described in [5], based on Set Membership (SM) approximation.

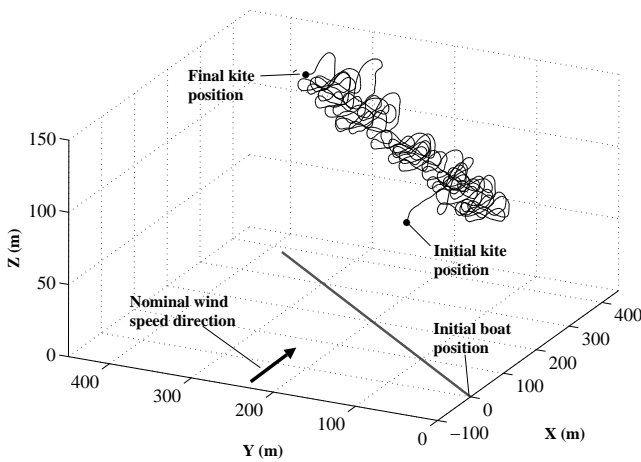


Fig. 6. Simulation results with $\Theta = 45^\circ$: paths of the boat (thick solid line) and of the airfoil (thin solid line).

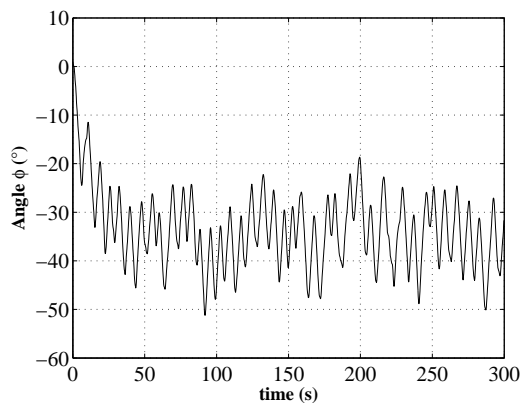


Fig. 7. Simulation results with $\Theta = 45^\circ$: course of angle $\phi(t)$.

IV. SIMULATION RESULTS

In the presented simulation tests, the nominal wind speed (1) is given by the following wind shear model:

$$W_n(Z) = \frac{\log\left(\frac{Z}{0.1}\right)}{\log\left(\frac{80}{0.1}\right)} 4.4 \quad (29)$$

Nominal wind speed is about 3.5 m/s at 20 m of altitude and grows to 4.5 m/s at 100 m of height. Moreover, uniformly distributed random wind turbulence \vec{W}_t has also been introduced, with maximum absolute value along each direction equal to 1 m/s, i.e. about 25% of the nominal wind speed at 100 m of altitude. The numerical values of model and control parameters introduced in Sections II–III are reported in Table I. Fig. 6 shows the obtained kite and boat trajectory, while

TABLE I
YO-YO CONFIGURATION: MODEL AND CONTROL PARAMETERS

m	3	Kite mass (kg)
A	10	Characteristic area (m ²)
d_l	0.0035	Diameter of a single line (m)
ρ_l	970	Line density (kg/m ³)
$C_{D,l}$	1	Line drag coefficient
α_0	3.5	Base angle of attack (°)
ρ	1.2	Air density (kg/m ³)
M	12	Boat mass (t)
Θ	45	Boat direction (°)
Δ_t	0.2	Sample time (s)
N_c	1	Control horizon (steps)
N_p	10	Prediction horizon (steps)
θ	70°	State constraint
ψ	10°	Input constraints
$\dot{\psi}$	40 °/s	

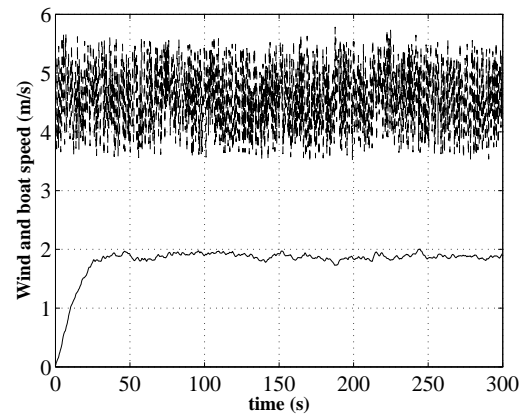


Fig. 8. Simulation results with $\Theta = 45^\circ$: courses of wind speed magnitude at the kite location (dashed line) and of the boat speed (solid line).

Fig. 7 shows the course of angle ϕ (which roughly gives the position of the kite with respect to the boat direction). It can be noted that, after the initial transient, the average value of ϕ is $\bar{\phi} = -35^\circ$, i.e. $\bar{\phi} \simeq -\Theta$: this result is consistent with the optimality analyses carried out in [4], thus showing that the controller employed here is able to effectively command

the kite flight in order to maximize the traction force, even in the presence of quite strong turbulence. The course of the boat speed is depicted in Fig. 8, together with the wind speed magnitude at the height where the kite flies. The boat speed reaches a steady state value of about $\tilde{v} = 1.9$ m/s, with small oscillations due to the kite movement and wind turbulence, while the average wind speed at the kite altitude is $\tilde{W} = 4.58$ m/s. Considering that a quite small kite is employed (i.e. 10 m² area), this result confirms the great potential of wind power generation using airfoils. Furthermore, the courses of the cable traction forces and of the kite speed magnitude $|\vec{W}_a|$ are shown in Fig. 9 and 10 respectively. The maximal traction force acting on each cable is about $1.8 \cdot 10^3$ N (i.e. about 15% of the breaking force of $1.2 \cdot 10^4$ N), while the average kite speed magnitude is equal to 16.13 m/s. Finally, according to the simulation results, the average kite efficiency is equal to 8.41, while the average overall efficiency (i.e. taking into account the cable drag, see [4]) is $\tilde{E} = 6.41$. The average value of θ is $\tilde{\theta} = 62^\circ$. The obtained results are consistent with the simplified formulation of average kite speed as a function of the projection of the effective wind speed along the cable direction (see e.g. [11]):

$$|\vec{W}_a| \simeq \left(\tilde{W} \cos(\tilde{\phi} + \Theta) - \tilde{v} \cos(\tilde{\phi}) \right) \sin(\tilde{\theta}) \tilde{E} = 16.8 \quad (30)$$

In the next Section, the obtained numerical results will be compared to the data collected in the first experimental tests carried out in the KiteNav project at Politecnico di Torino.

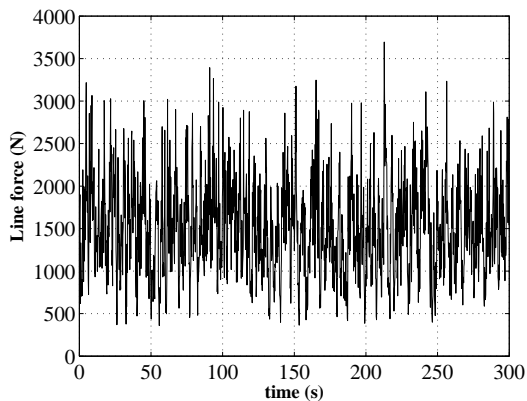


Fig. 9. Simulation results with $\Theta = 45^\circ$: course of the overall traction force acting on the cables.

V. EXPERIMENTAL TESTS

The experimental data shown in this section is part of the measures collected during field tests performed near Varazze, Italy, in July 2009 (see Fig. 11). A movie of the experimental test is also available [12]. During the test, a wind of 2 m/s on average was present at sea level. The employed kite had an effective area of 10 m². A GPS was installed both on the kite and on the boat, moreover the kite was equipped with a magnetometer, three gyroscopes and three accelerometers in order to measure its position, speed and orientation. Fig. 12 shows the measured trajectories of the boat and the kite

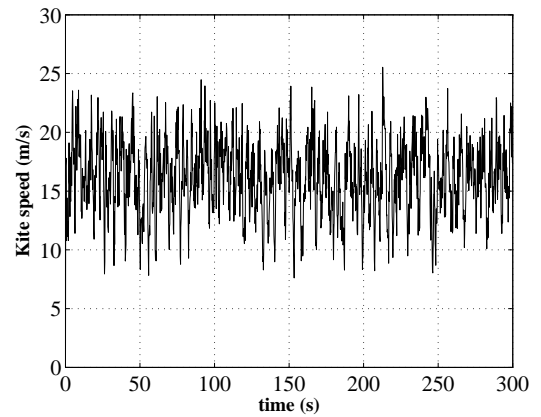


Fig. 10. Simulation results with $\Theta = 45^\circ$: course of the kite speed magnitude $|\vec{W}_a|$.

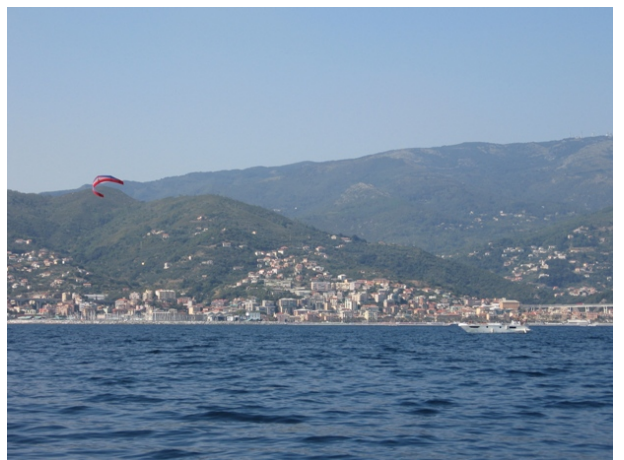


Fig. 11. (KiteNav project, picture of the experimental test carried out near Varazze (Italy), in July 2009)

during part of the tests, while Fig. 13 and 14 show the courses of the boat speed and of the kite speed respectively. The kite flight was commanded by a human operator through two joysticks that allow to set reference values of torque and differential cable length for the electric drives of the KSU. Thus, the obtained kite trajectories were not optimal; however, according to equation (30) the experimental results are quite consistent with the numerical results obtained using the NMPC approach and presented here, giving a good confidence level in the accuracy of the employed model and in the obtained simulation results. In fact, the average measured speed value of the boat was $\tilde{v} = 1.2$ m/s, the average measured values of angles θ and ϕ were $\tilde{\theta} = 70^\circ$ and $\tilde{\phi} = -72^\circ$ respectively, the angle between the boat path and wind direction was about 90° and the estimated wind speed at the kite altitude (i.e. 120 m above sea level) was about 2.5 m/s. Applying equation (30), the computed value of the kite speed magnitude is 10.45 m/s. Such a value matches with the average measured kite speed of 10.9 m/s.

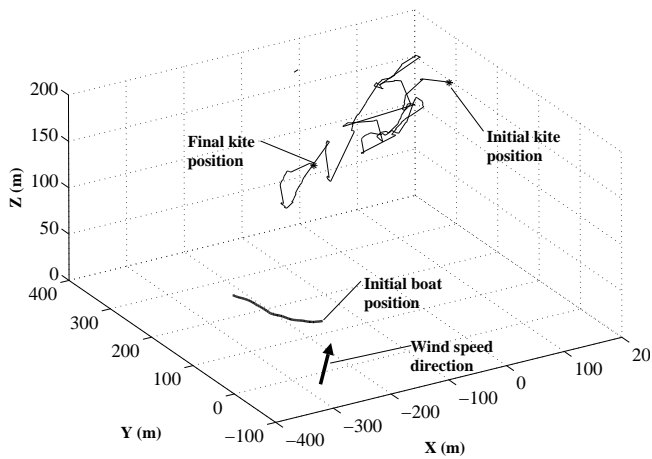


Fig. 12. KiteNav project, experimental test carried out near Varazze (Italy), in July 2009: measured paths of the boat (thick solid line) and of the airfoil (thin solid line).

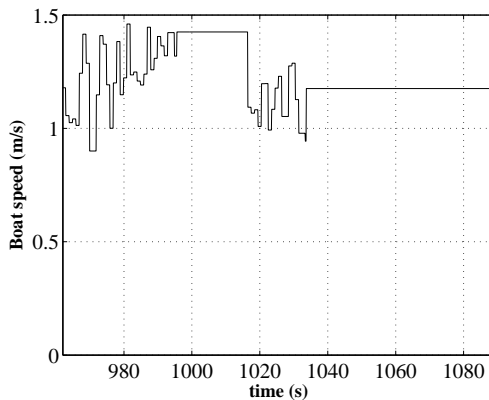


Fig. 13. KiteNav project, experimental test carried out near Varazze (Italy), in July 2009: measured course of the boat speed v .

VI. CONCLUSIONS AND DEVELOPMENTS

The paper presented simulation and experimental results regarding an application of high-altitude wind power using power kites to naval propulsion. A model of the boat and the kite has been introduced and a NMPC law has been employed to maximize the traction force acting on the boat, while satisfying operational constraints. Moreover, the results of the first experimental tests carried out at Politecnico di Torino in the KiteNav project have been also presented, showing a good consistency with the numerical results. The next objectives of the project are the use of experimental data in order to assess and improve the accuracy of the employed mathematical model and the design, implementation and experimental testing of a reliable and efficient automatic control law.

REFERENCES

[1] M. Canale, L. Fagiano, and M. Milanese, "High altitude wind energy generation using controlled power kites," *IEEE Transactions on Control Systems Technology*, in press. doi: 10.1109/TCST.2009.2017933.

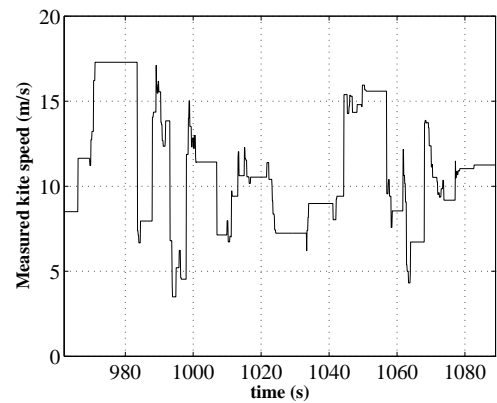


Fig. 14. KiteNav project, experimental test carried out near Varazze (Italy), in July 2009: measured course of the kite speed magnitude $|\vec{W}_a|$.

- [2] A. Ilzhöfer, B. Houska, and M. Diehl, "Nonlinear MPC of kites under varying wind conditions for a new class of large-scale wind power generators," *International Journal of Robust and Nonlinear Control*, vol. 17, pp. 1590–1599, 2007.
- [3] SkySails GmbH & Co., <http://www.skysails.info>.
- [4] B. Houska and M. Diehl, "Optimal control of towing kites," in *45th IEEE Conference on Decision and Control*, San Diego, CA, 2006, pp. 2693–2697.
- [5] M. Canale, L. Fagiano, and M. Milanese, "Set Membership approximation theory for fast implementation of model predictive control laws," *Automatica*, vol. 45, no. 1, pp. 45–54, 2009.
- [6] C. L. Archer and M. Z. Jacobson, "Evaluation of global wind power," *J. Geophys. Res.*, vol. 110, D12110, 2005.
- [7] National Oceanic & Atmospheric Administration – Earth System Research Laboratory, NOAA/ESRL Radiosonde Database Access: <http://raob.fsl.noaa.gov/>.
- [8] M. Diehl, "Real-time optimization for large scale nonlinear processes," Ph.D. dissertation, University of Heidelberg, Germany, 2001.
- [9] B. Houska and M. Diehl, "Optimal control for power generating kites," in *9th European Control Conference*, Kos, GR, 2007, pp. 3560–3567.
- [10] D. Q. Mayne, J. B. Rawlings, C. V. Rao, and P. Scokaert, "Constrained model predictive control: Stability and optimality," *Automatica*, vol. 36, pp. 789–814, 2000.
- [11] L. Fagiano, "Control of tethered airfoils for high-altitude wind energy generation," Ph.D. dissertation, Politecnico di Torino, Italy, February 2009, available on-line: http://lorenzofagiano.altervista.org/docs/PhD_thesis_Fagiano_Final.pdf.
- [12] KiteNav project, Politecnico di Torino. Experimental test movie, July 2009. Available on-line: http://lorenzofagiano.altervista.org/movies/KiteNav_Varazze_test.wmv.